Program Digest, 2019 IEEE International Ultrasonics Symposium (IUS)
Glasgow, Scotland, October 6-9, 2019

Deformation Independent Non-linearity Estimation: Studies and Implementation in Ultrasound Shear Wave Elastography

Soumya Goswami, Siladitya Khan, Rifat Ahmed, Marvin M. Doyley and Stephen A. McAleavey
Hajim School of Engineering and Applied Sciences
University of Rochester
Rochester, NY, USA
sgoswam2@ur.rochester.edu

***Abstract*—Nonlinear elasticity imaging provides additional information about tissue behavior that is potentially diagnostic and can lead to better tissue characterization. Nonlinear elastic properties of tissue become apparent upon application of large deformation to the medium. The majority of nonlinear elasticity estimation techniques rely on uni-axial compression. Here, we study the change in shear wave speed with the medium subjected to simple shear stress and also pure uniaxial compressive stress. Axial and lateral deformation of the tissue was tracked using quasi-static strain elastography. The local stress map is computed from cumulative sum of apparent shear modulus (measured by shear wave elastography) times the estimated differential strain. By fitting the change in local stress obtained to the estimated strain, nonlinear shear modulus is mapped. The rate of the change in local stress distribution in the medium differs with different deformations applied. However, the absolute value of nonlinear shear modulus obtained for different deformations applied were similar, thereby demonstrating the ability to give a quantitative measure of material non-linearity irrespective of subjected deformations.**

***Index Terms*—shear wave elastography, shear strain, nonlinear elasticity, shear wave speed, tissue deformation**

I. Introduction

Nonlinear mechanical properties of tissues such as shear nonlinearity, viscoelastic nonlinearity, geometric nonlinearity and others are important in numerous biological functions as well as clinical diagnosis [1]. Linear elastic tissue models are assumed in most of the ultrasound elasticity imaging approaches. Measurement of nonlinear elastic properties provides additional information about tissue but such measurements are challenging. Large deformations are required for the tissue to exhibit its nonlinear property as shown in Fig. 1. Material tracking methods are required to track the large deformation of the tissue and register material properties obtained in the deformed state with the original, undeformed structure [2].

Several groups have used quasi-static elastography to determine the slope of the stress-strain curve and imaged the nonlinear parameter as the rate at which the curve departs from linear behavior [3]. However, this estimate is dependent on the nature of induced deformation. In this study we see that with uni-axial compression and simple shearing, different estimates of slope of stress-strain curve are obtained for a similar soft tissue material. A nonlinear shear modulus parameter that is independent of applied tissue deformation has been studied. Imaging of the nonlinear shear modulus gives the same absolute value of nonlinear elasticity for both simple shearing and uniaxial compression.

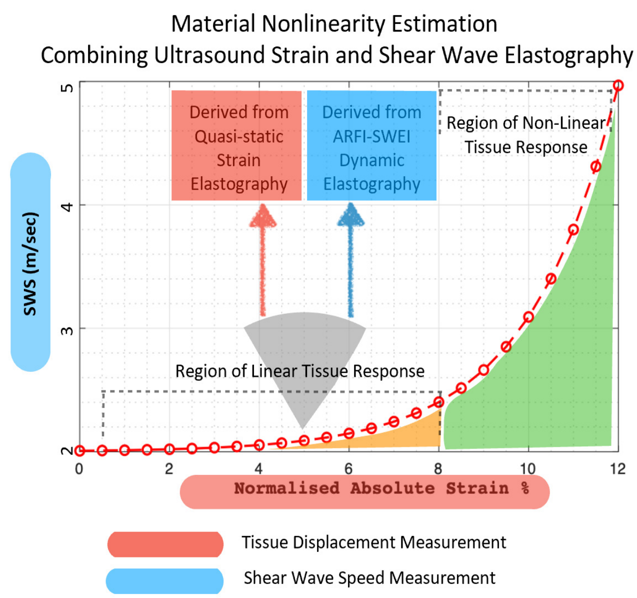

Fig. 1. Demonstration of stress-strain curve with linear region marked yellow and nonlinear region in green. Strain data will be measured by quasi-static elastography and shear wave data with dynamic elastography. Nonlinearity is apparent with higher deformations.

II. Materials and Methods

To estimate the shear wave speed changes as a function of strain, small progressive deformations to the tissue (simple shear or uniaxial compression) were given at multiple levels. At each deformation step, RF echo data were acquired. 2-D cross-correlation was used to estimate the axial and lateral deformation vectors between pre and post compression RF data [4]. The estimated two-dimensional deformation vectors

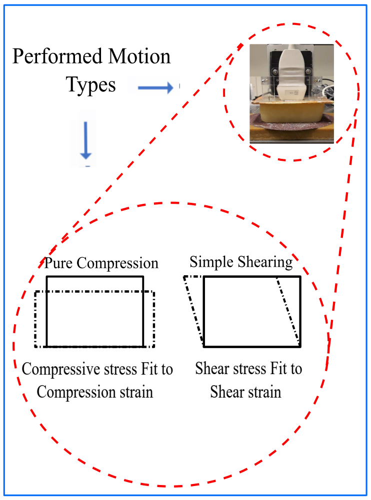

Fig. 2. Experimental setup for NLSM imaging. A compression plate attached to the transducer. Two sand papers, one in between plate and tissue and one at the bottoms ensures no slipping condition. Two deformation types were shown.

at each step were registered with respect to the initial undeformed state of the material. From the registered deformation vectors [5], the axial and shear strain were estimated. The corresponding shear wave speed map was obtained by single track location shear wave elasticity imaging (STL-SWEI) [6] at each deformation step. The linear shear modulus (μ) is calculated by using:

$$\mu = \rho \cdot V_S^2 \quad (1)$$

where ρ is medium density, and V_S is the shear wave speed. The local stress at the i^{th} compression step is estimated from the cumulative sum of incremental local strain times the apparent shear modulus at each deformation step as given by:

$$\sigma_i = \sum_{j=1}^{i} 3\mu_j \Delta\epsilon_j \quad (2)$$

$\Delta\epsilon_j$ is the differential strain (axial or shear strain as required) estimated at each deformation step following registration of the tissue motion from estimated axial and lateral displacements. By fitting the measured apparent shear modulus values to the stress estimated at each deformation steps, the nonlinear shear modulus (NLSM) A is obtained.

All imaging experiments were performed using a ATL L7-4 linear array driven by a Verasonics Vantage 64LE ultrasound system (Verasonics Inc., Kirkland, WA, USA). A compression plate (9cm x 5.5cm) was attached to the transducer, itself mounted on a 5-axis position controller to give controlled deformation in between each levels. Sand paper was applied to the compression plate surface and table surface to prevent slipping of the phantom under lateral shear.

Raw channel data were acquired at a ultrasound frequency of 5 MHz, 60% bandwidth. At each deformation step, data were acquired from successive plane wave transmissions at forty different transmission angles between $-7°$ and $7°$. Plane wave coherent compounding was applied to improve estimation of lateral motion. Delay-and-sum (DAS) beamforming implemented on a graphics processing unit (GPU) was applied to the raw channel data. During the beamforming, a dynamic receive F# of 1.5 was applied. Beamforming was implemented on a uniform grid with 240 axial points and 128 lateral points covering 36mm and 18.5 mm, respectively.

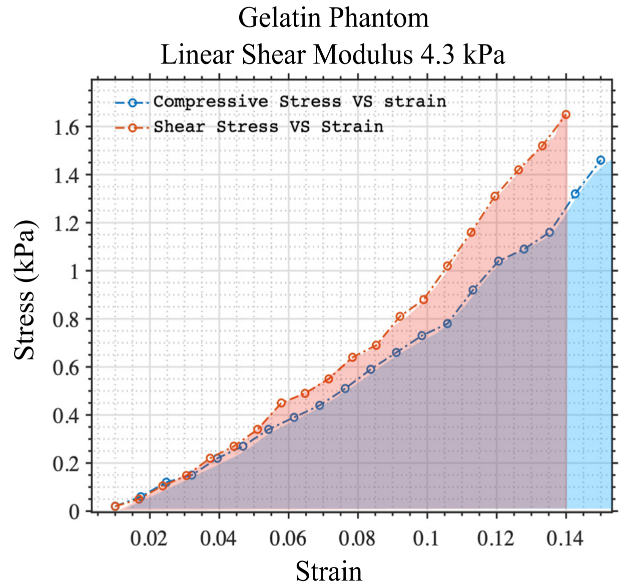

Fig. 3. Experimental Stress-strain curve for a 4.3 kPa homogeneous phantom. Shearing stress-strain (marked in red) has high slope compared to compressional shear-strain slope (marked in blue). This mandates a more generic closed form nonlinearity measure

III. Results

Fig 3. shows stress-strain curve obtained for simple shearing deformation (marked red) and uniaxial compression (marked blue) at different strain levels for a 4.3 kPa gelatin homogeneous phantom. The slope of stress strain curve is same for both deformation types upto 5% strain. Further the stress strain curve is linear upto 5% strain. At higher strain, the shearing stress-strain curve has greater slope compared to axial stress-strain curve. Thus the rate of departure of slope of stress-strain curve from linearity cannot be exclusively used as a quantitative nonlinear parameter. Fig. 4 demonstrates the NLSM map obtained for the same homogeneous gelatin phantom both by compression and shearing. The absolute value of NLSM obtained were 51.4 kPa and 53 kPa for uniaxial compression and simple shearing respectively. The error estimates of NLSM fitting converges to zero at higher strain as shown in Fig. 4 (D). This suggests that with more fitting data points and higher strain NLSM estimates converge.

For an inclusion phantom of 18kPa in 5kPa background as shown in Fig. 5, the contrast obtained in nonlinear elastograms were much higher compared to that obtained in linear elastograms. There is good correspondence between absolute values of NLSM obtained by simple shearing and uniaxial compression.

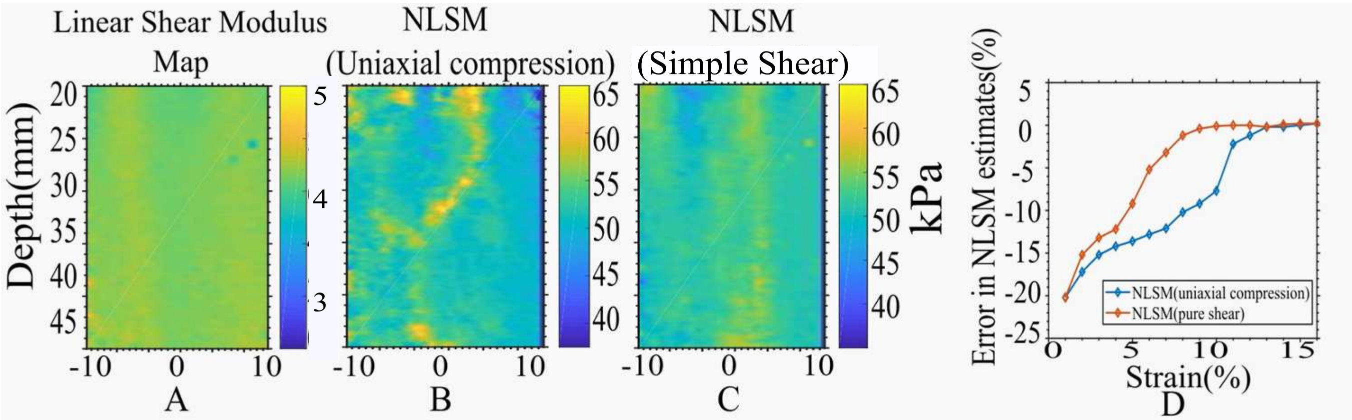

Fig. 4. Representative Linear Shear Modulus Map, NLSM map by compression and shear respectively for a 4.3 kPa homogeneous phantom. (D) Error Estimates of NLSM converges with strain.

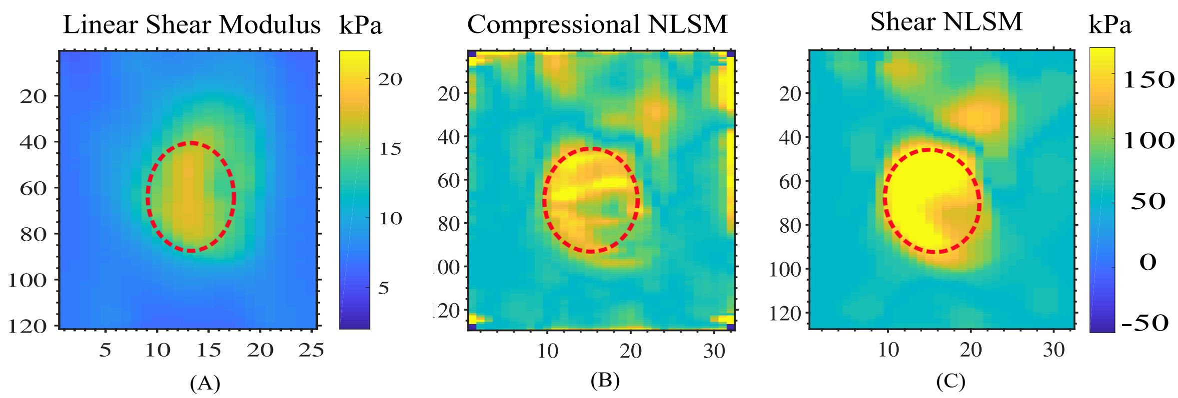

Fig. 5. Experimental NLSM imaging. (A) Linear Shear Modulus Map of 18kPa inclusion in 5 kPa background. (B) NLSM map by uniaxial compression (C) NLSM by simple shear. The absolute NLSM value of inclusion matches for simple shearing and compression..

IV. Discussion

In this study we combined quasi-static and shear wave elastography to estimate the local stress distribution within the medium following uni-axial compression and simple shearing. We find that the slope of the stress-strain curve is dependent on the type of deformation applied to the tissue. To address this issue, we explored the ability of our NLSM estimate to provide consistent values irrespective of deformation applied. The absolute value of NLSM agrees for different deformation types for both homogeneous and inhomogeneous tissue mimicking phantoms.

Future studies are needed to improve the reconstruction and resolution of the NLSM maps. Further, here controlled deformations were given in multiple levels. Adapting this method to handheld deformations applied instead of controlled deformations will increase its utility. Future efforts would be directed towards theoretical relations between shear wave speed changes with incremental strains. Further, there might be slip issues while giving high deformations which can be minimized with a robotic control arm [7].

Acknowledgment

This work was supported in part by the Office of the Assistant Secretary of Defense for Health Affairs through the Breast Cancer Research Program under Award No. W81XWH-17-1-0021. This work was also supported by NIH grant 5R21EB017503-02.

Conclusion

We found that the change in shear wave speed with strain varies with the nature of the deformations. The behavior of the local stress estimates derived from apparent shear modulus and differential strain varies with type of deformations applied. A novel 2-D motion registered nonlinear shear modulus estimation technique has been proposed to measure the shear nonlinearity of soft tissues. NLSM imaging gives same absolute value of non-linear elasticity for simple shearing and uni-axial compression, and gives high contrast elastograms compared to linear shear modulus images.

References

[1] J.-L. Gennisson, S. Catheline, C. Bari, J. Bercoff, M. Tanter, and M. Fink, “Acoustoelasticity in soft solids: Assessment of the nonlinear shear modulus with the acoustic radiation force,” J. Acoust. Soc. Am., vol. 122 no. 6, pp. 3211-3219, 2007.

[2] Goswami, Soumya and Ahmed, Rifat and Doyley, Marvin M and McAleavey, Stephen A, "Nonlinear Shear Modulus Estimation with Biaxial Motion Registered Local Strain," IEEE Trans. Ultrason., Ferroelect., Freq. Control, vol. 66, no. 8, pp. 1292-1303, Aug. 2019.

[3] Oberai, A. and Gokhale, N. H. and Goenezen, S. and Barbone, P. E. and Hall, T. J., Sommer, A. M. and Jiang, J., "Linear and nonlinear elasticity imaging of soft tissue in vivo: demonstration of feasibility," Physics in Medicine & Biology, vol. 54, no. 5, pp. 1191, 2009.

[4] M. M. Doyley "Model-based elastography: A survey of approaches to the inverse elasticity problem," Phys. Med. Biol., vol. 57 no. 3 pp. R35-R73 Jan. 2012.

[5] Goswami, Soumya and Ahmed, Rifat and Doyley, Marvin M and McAleavey, Stephen A, "2D tracking improves quantitative nonlinear shear modulus estimation," Ultrasonic Imaging and Tissue Characterization Symposium Abstracts 2019. (2019). Ultrasonic Imaging, 41(3), 131172. https://doi.org/10.1177/0161734619842019

[6] E. Elegbe, and S. McAleavey, "Single tracking location methods suppress speckle noise in shear wave velocity estimation," Ultrasonic Imaging., vol. 35, no. 2, pp. 109-125,2013.

[7] M. E. Napoli, C. Freitas, S. Goswami, S. McAleavey, M. Doyley and T. M. Howard, "Hybrid Force/Velocity Control With Compliance Estimation via Strain Elastography for Robot Assisted Ultrasound Screening," 7th IEEE International Conference on Biomedical Robotics and Biomechatronics (Biorob), Enschede, 2018, pp. 1266-1273.